Torus doubling resonances and breather stability

L. S. Schulman[*]

Physics Department, Clarkson University, Potsdam, New York 13699-5820, USA
and Max Planck Institute for the Physics of Complex Systems, Nöthnitzer Strasse 38, D-01187 Dresden, Germany

E. Mihóková[†]

Institute of Physics, Academy of Sciences of the Czech Republic, Cukrovarnická 10, 162 53 Prague 6, Czech Republic

Discrete breathers that arise in doped alkali halides lead us to study two properties of these localized excitations. First, we note a bifurcation phenomenon, which we dub *torus doubling*, in which resonant coupling in the nonlinear modes induces a period doubling of the phase space structure. Second, we find that although two-frequency breather excitations are not in principle localized (because of phonon resonances), in practice they can survive 10^9 times the characteristic time scale and give rise to marked physical phenomena, including the one that brought us to this study, the anomalous decay of luminescence.

PACS number(s): 05.45.−a, 63.20.Ry, 31.70.Hq, 63.20.kp

I. INTRODUCTION

To explain the anomalous decay of luminescence in certain doped alkali halides [1–5], we have invoked the creation of discrete breathers. As the result of investigating these breathers, we report two phenomena, one of general interest in the theory of nonlinear dynamical systems and the other providing further theoretical support to our model. The first phenomenon is the *bifurcating torus*. Bifurcations associated with period doubling one-dimensional orbits (loops) have been observed in many phenomena. In our case, one already has a torus, and it is this torus that undergoes period doubling in a way that relies on the presence of both modes. Demonstrating the period doubling is aided by an extension of the method of sections, since an additional dimensional reduction is useful. The second phenomenon is the stability of the breather in our physical system despite the in-principle existence of destabilizing factors.

For specificity we discuss KBr:Pb^{2+}. The doped crystal is illuminated by a UV pulse and in the neighborhood of the Pb there is Jahn-Teller-effect symmetry breaking with a large distortion, especially along the symmetry-breaking crystal axis. The resulting force creates a breather adjacent to the impurity site. The natural time scale of the crystal relaxation is picoseconds and the breather holds on to the distortion energy for an enormously long time—milliseconds. This leads to the decay anomaly, as explained in [6–8].

Mathematically, discrete breathers in one-dimensional *monatomic* lattices have been shown to exist [9,10]. However, one expects that in a diatomic lattice the presence of two frequencies at which significant oscillation takes place would cause resonances and destroy the breather. (One breather frequency is above the optical phonon spectrum of the lattice, while the other is in the gap between the acoustical and optical phonon bands.)

In this paper we provide evidence for the survival of our breathers on the scale necessary for the explanation of the experimental data, namely, 10^9 natural lattice time units, more than 10^8 breather oscillations. It is remarkable that one can reach this conclusion on the basis of runs of a few thousand time units.

Of further interest, with respect to the general understanding of nonlinear phenomena, is the behavior of our system in the neighborhood of a resonance. One might have thought this to be particularly dangerous to the survival of the breather, but what we see instead is what we believe to be a new kind of bifurcation. Below the resonance (in a certain control parameter), the system lives on a torus in phase space. As the critical region is approached there is a period doubling, just as for an ordinary orbit, but with the entire torus doubled. Once the resonance has passed (as a function of the control parameter), the system goes back to the usual torus. Now one could certainly see a torus bifurcation if a system with a loop-orbit bifurcation had attached to it a noninteracting or perhaps weakly interacting oscillator. But in our case both dimensions of the torus are inextricably intertwined and one could not reduce our torus to a loop while maintaining the bifurcation. It should be noted however that our demonstration is entirely numerical, and we have not provided a mathematical proof of a singularity.

After reviewing our notation and methods in Sec. II, we reverse the order of presentation of this introduction and in Sec. III display, with detailed images, the bifurcation associated with a period doubling in the torus dynamics. The next section, Sec. IV, deals with stability: despite the possibility of breather coupling to phonons through nonlinear forces, the system is nevertheless stable on remarkably long time scales. The last section presents a discussion and conclusions.

II. BACKGROUND AND NOTATION

We focus on KBr:Pb^{2+}, although there are several other crystal matrices as well as impurities in which anomalous decay is observed. In the experiments [1–5], a UV flash excites the impurity (Pb). The center, consisting of the impurity and its nearest neighbors, undergoes a symmetry-breaking distortion (the Jahn-Teller effect) along a particular axis. We
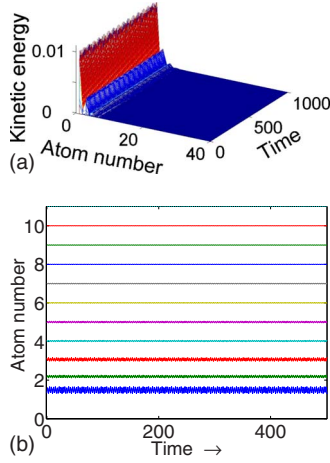
*schulman@clarkson.edu
†mihokova@fzu.cz

FIG. 1. (Color online) Kinetic energy and atom positions as a function of time for a breather obtained by integrating the equations of motion for the Hamiltonian (1). The parameter values are $\lambda = 1$, $\nu = 1$, $r = 2$, and $q_0 = 0.4791$. We took $q_k = Q_k = \dot{q}_k = \dot{Q}_k = 0$, $k \geq 1$ as initial conditions for all atoms (but the nondynamical $q_0 > 0$) and imposed absorption near atom-40. After 1500 time units the absorption was discontinued and the resulting state became the initial conditions for the above figure. In addition there is a slight departure from the Hamiltonian (1) in that the masses of the atoms near the outer boundary were slightly randomized, thereby destroying coherent reflections through Anderson localization. The units are indicated in the text.

model the crystal along this axis. Using reflection symmetry, the model becomes a one-dimensional diatomic chain with a large force applied at one end (due to the Pb distortion) [11]. The Hamiltonian is

$$H = \sum_{n=1}^{N} \left(\frac{P_n^2}{2M} + \frac{r p_n^2}{2M} + V(q_n - Q_n) + V(Q_n - q_{n-1}) \right.$$

$$\left. + \nu [V(Q_n) + V(q_n)] \right). \tag{1}$$

Q_1 is the Br ion to the right of the Pb, followed by q_1 (a K ion), Q_2, etc. The Q particles have mass M, the q's, M/r. The expression multiplying ν provides a substrate or holding force, required by our restriction to one dimension. For KBr, $r \approx 2$. This Hamiltonian, describing only Br and K, includes the effect of the highly distorted Pb wave function through the nondynamic variable q_0. By setting this to specific positive values we can provide a push on the entire chain, inducing intense oscillation, possible breather formation, and possible wave propagation, depending on the model parameters. The potential is $V(u) = M\omega_0^2(u^2 + \lambda u^4)/2$. A quadratic potential would not be adequate because the Jahn-Teller distortion is known to induce a displacement of up to 15% or 20% of the ionic spacing. We adjust units so that both M and ω_0 are 1. The time scale is thus approximately picoseconds. See the Appendix in Ref. [12] for a detailed discussion of units.

As an illustration, in Fig. 1 we show the kinetic energy as a function of time for parameter values close to those used in much of the present paper. In [12] we considered other forms

of V, but we now confine attention to the quartic with $\lambda > 0$.

III. PERIOD DOUBLING TORI

Phase space structures for nonlinear systems are famously complex [13], with the concepts of bifurcation and period doubling playing an important role. As we now show, both of these occur in our system, but because of the dimension of the structure we cannot use the most direct kind of Poincaré section to illustrate the phenomena. On the other hand, the dimension is not so high that our bifurcation should be rare.

We will refer to the phenomenon as *torus doubling*, since the phase space structure consists of a torus that passes through itself, at least when thought of as a subset of three-space. We have established, however, that on a full loop of the doubled torus, orientation is preserved.

For the present discussion, the parameters of the Hamiltonian, Eq. (1), are fixed. (We take $\lambda = 1$ and $\nu = 1$, while M and ω_0 are 1 by virtue of the units.) The control parameter is q_0, the force on the first atom due to the Jahn-Teller effect.

To give an overview, in Fig. 2 we show phase space structures for various values of q_0. What is illustrated is the points $(Q_1(t), \dot{Q}_1(t), q_1(t)) \subset \mathbb{R}^3$ for $t = n\Delta t$, $n = 1, 2, \ldots, N$, $N = T/\Delta t$ with $T \sim 5000$ and Δt usually taken to be 0.1. For small q_0 one gets a thin torus, while for large q_0 one also gets a torus, but with larger radii. In the intermediate region, near $q_0 = 0.5$, there is a period doubling, with the center of the torus forming a curve approximately twice the length of the unsplit loop.

A detailed investigation reveals the following points.

(i) The dominant frequency for $q_0 \lesssim 0.47$ is the breather frequency in the gap between the acoustic and optical phonons. This will be called ω_ℓ (for "low"). The other breather frequency, that above the optical band, to be called ω_h ("high"), has smaller, but nonzero amplitude.

(ii) In the neighborhood (with respect to q_0) of the torus doubling, the ratio of ω_h to ω_ℓ is close to 3 to 2. This implies that the half frequency, that which is associated with period doubling, is increasingly excited by nonlinear terms in the equation of motion. As a resonance, this is the lowest possible order (1-1), with $\omega_h - \omega_\ell \sim \omega_{pd}$, where $\omega_{pd} = \omega_\ell/2$ is the period-doubling frequency.

(iii) Fourier transforms of the positions of the first four atoms confirm the excitation of the period doubling frequency; interestingly, there is greater amplitude for the half frequency ($\omega_\ell/2$) in the second atom than in the first. The small low frequency bump in the transform of atom 2 for $q_0 = 0.4$ seen in Fig. 3 is neither at the half frequency of ω_ℓ nor at the difference frequency of the main breather frequencies. As q_0 increases, a bump develops near the difference frequency, and as we approach the regime of period doubling, that difference begins to coincide with the half frequency.

(iv) The double loop is not knotted.

(v) Close to exact matching of the frequency ratio, one requires very long computer runs to see the torus fill out. For shorter times one gets a closed ribbonlike structure. By checking the orientation of lines on cross sections of the
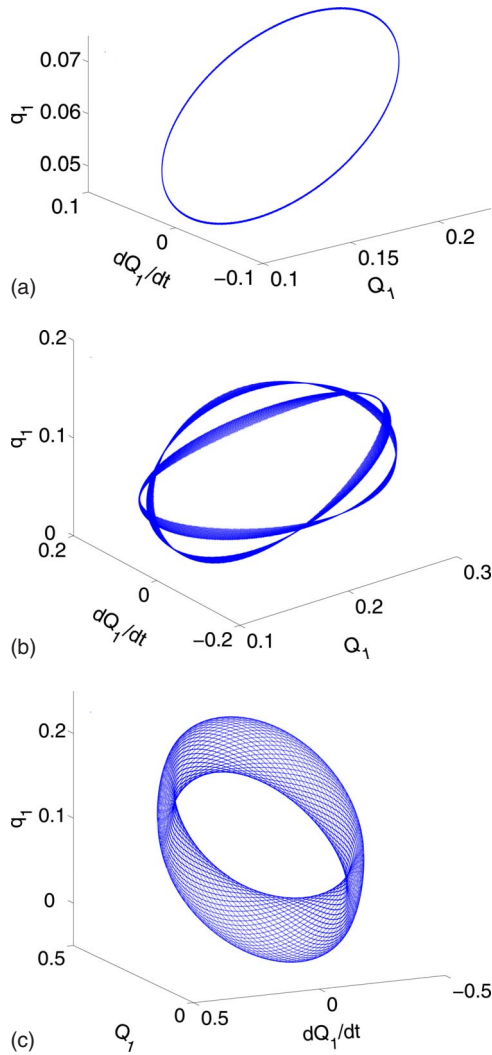
FIG. 2. (Color online) Phase space structures for $q_0 = 0.4$, 0.498 25, and 0.59.

FIG. 3. (Color online) Frequency spectra of the first 4 atoms for $q_0 = 0.4$, 0.49825 and 0.59 [(a), (b), and (c), respectively]. (Atom no. 2's spectrum is displaced by four units below that of atom no. 1, etc.) The green bands traversing the figures vertically represent the phonon bands (acoustic and optical).

ribbon, we found that the orientation does not change, i.e., it is a cylinder and not a Möbius strip.

(vi) For longer runs, the portion of the loop formed in the second half of the doubled period nearly overlaps with the first. By averaging over successive cross sections however, one can see that this averaged quantity behaves like the doubled orbit in lower dimensional period doubling orbits (e.g., for the Duffing equation, [14], Fig. 11-7, or the Rössler equation, [15], Fig. 3).

(vii) It is important to distinguish the doubled torus from a 3-2 ratio Lissajous figure. With a ratio close to (but not exactly) 3-2 and for runs of finite length, such a figure can indeed resemble Fig. 2(b). Nevertheless a sharp distinction can be drawn by stroboscopic cross sections with varied time intervals.

(viii) The same phenomenon occurs for $\nu = 0.75$ for q_0 near 0.59, indicating that torus doubling is generic.

(ix) As remarked in the Introduction, the period doubling of our torus is not simply the doubling of a one-dimensional
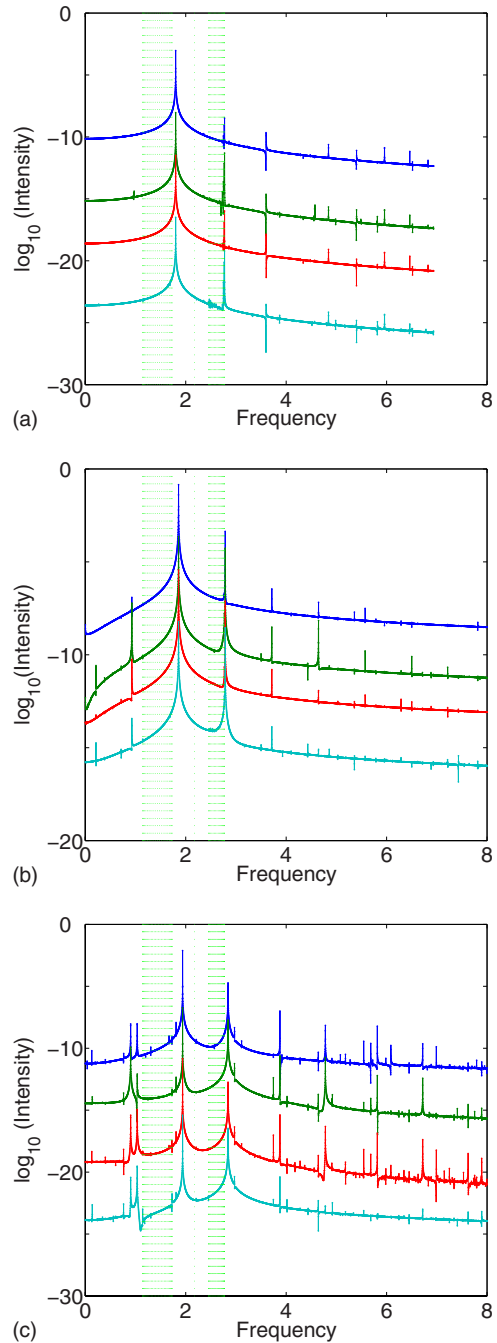
orbit, fattened by an extra oscillator. By adjusting additional control parameters one can indeed suppress one or the other breather frequency [16]. However, the essence of this bifurcation is a 3-2 resonance involving *both* these modes, depending thereby on the nonlinear coupling. Hence the phenomenon studied here intrinsically depends on the full torus structure.

We elaborate on these points.

A. Frequencies and their ratios

In Fig. 3 we show the Fourier spectra (intensities) for the motion of the first four particles for three values of q_0. For $q_0 = 0.4$, ω_h barely exceeds the top of the optical spectrum and is much reduced in amplitude relative to ω_ℓ. For Fig. 3(b) $q_0 = 0.4968$ and ω_h has strengthened relative to what was seen in Fig. 3(a). But the significant point is the presence of relatively high intensity at lower frequencies. The frequency maxima are (0.9289, 1.8577, 2.7852). Keeping additional significant figures, it turns out that these are in the ratio (to ω_ℓ) $(1/2 + 5 \times 10^{-6}, \ 1, \ 3/2 - 7 \times 10^{-4}, \ 5/2 - 2 \times 10^{-5})$. The half frequency, of course, indicates period doubling, and from the figure one notes that it is mainly atom no. 2 that experiences this effect (relatively speaking—the 3rd and 4th atoms also have large half-ω_ℓ contributions, but their overall amplitude is small). For Fig. 3(c) ($q_0 = 0.59$), it is clear that many harmonics of the breather frequencies are generated. The relatively large contributions just below the acoustical band are *not* at the half frequency of ω_ℓ and do not have the same destabilizing effect as the corresponding amplitude for $q_0 = 0.4968$. In this case the important frequencies are (0.9041, 1.0343, 1.9384, 2.8425, 2.9723, 3.8768, 4.7809). To a good approximation these are $(\omega_h - \omega_\ell, \ 2\omega_\ell - \omega_h, \ \omega_\ell, \omega_h, \ 3\omega_\ell - \omega_h, \ 2\omega_\ell, \ \omega_h + \omega_\ell)$.

B. Knots and topology

For the doubled loop our images are three-dimensional plots seen on the two-dimensional screen of a computer. To determine topological features we rotated the image using MATLAB® software. Regarding knots, the figure showed that the projected (on the screen) loop had five self-crossings, two pairs of which could be pulled back (ascertained by rotating and seeing what was in front of what), leaving a single crossing and an unknotted loop.

On close inspection, the image in Fig. 2(b) does not form a complete torus, but rather is a closed ribbon. What we next checked was whether it was a cylinder or a Möbius strip. We remark that the ribbonlike structure is present because of the near exactness of $\omega_h / \omega_\ell \approx 3/2$. This ribbon is the same as one gets by simply plotting appropriate combinations of sines and cosines, not derived from dynamics. By strobe plots to be described in more detail below, we put lines transverse to the ribbon at many places along its length (for many phases of the strobe). Careful examination showed that the orientation of this line did not change as one made one's way around the loop (which meant two circuits of what had been the unbifurcated torus); see Fig. 4.

C. Lowering dimension by stroboscopic averaging

For the torus, a stroboscopic view of the full phase space structure gives a loop, and this method was used extensively in [17] for semiclassical quantization of the breather. However, when the torus itself undergoes a bifurcation it is useful to supplement this technique with an averaging process.

The most straightforward way to see the doubling is by strobing at ω_h, since this will outline a loop of constant angle (in the sense of action-angle variables) of the motion of the
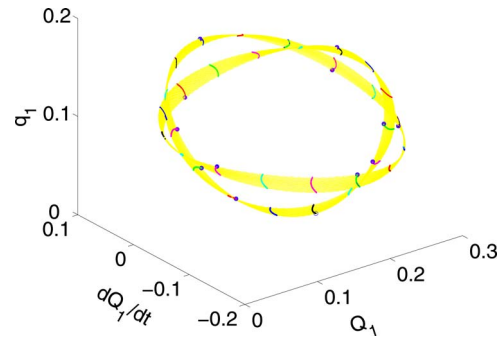

FIG. 4. (Color online) Transverse markings on the "ribbon" allowing its orientation to be checked.

other variable. This gives rise to two closely intertwined curves, which under high magnification can be separated; see Fig. 5. (As we discuss below, there is *no* such doubling for the Lissajous figure arising artificial data with a near-2-to-3 frequency ratio.) A second technique is to look at constant angle at the frequency associated with the period doubling, $\omega_\ell / 2$. This will give a loop along the other axis of the torus. Such loops would be seen in Fig. 4 if we were to run the simulation for long enough for the ribbon to close on itself (transversely). To see the bifurcation, it is not useful to fill in these loops densely, since they have considerable overlap with one another (but we will return later with a slightly
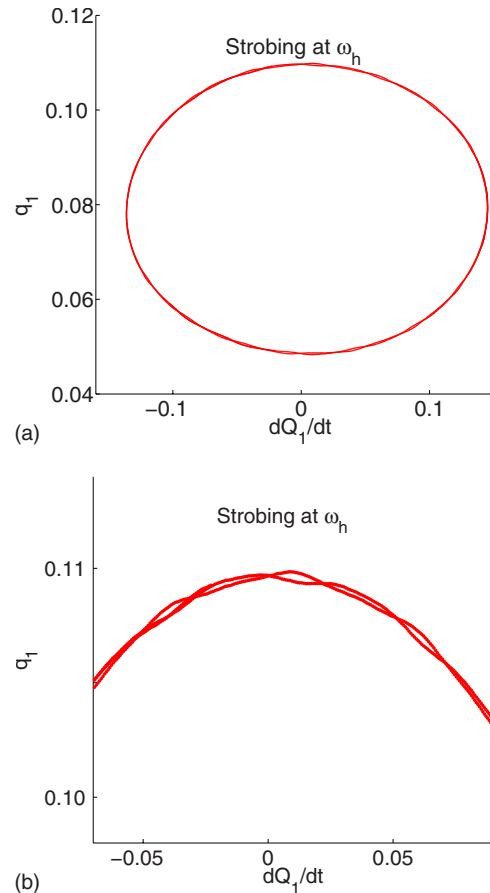

FIG. 5. (Color online) Strobing at ω_h, showing the double loop structure; $q_0 = 0.4791$. Both the entire image and a detail are shown.
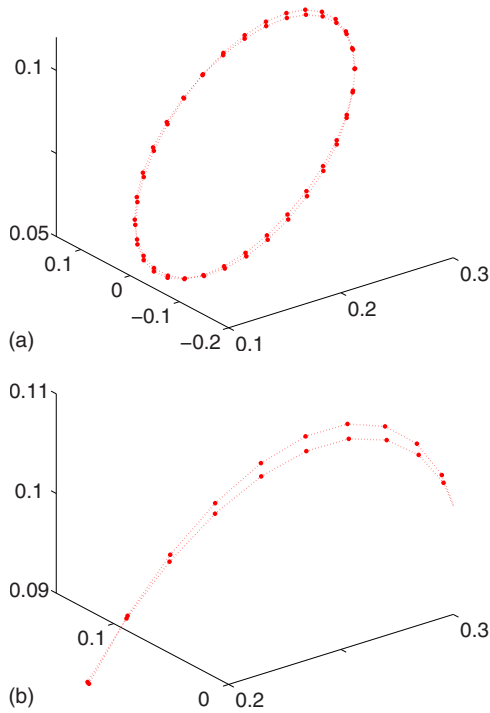
FIG. 6. (Color online) Averages of the center of cross sections of constant phase, showing the double loop structure. Both the entire image and a detail are shown.

refined variation of this method). Instead, for each such loop—which is a set of constant angle points—we averaged over its position, getting in effect a center of mass for a fixed phase. Collecting many such, a double loop of loop centers is traced out, and it becomes evident that the original torus has split into two. In Fig. 6 is shown the overall figure as well as a detail.

We next check that the period doubling we report is not merely a Lissajous figure with a 3-2 ratio. This is an important point, since superficially the image of such an object with a ratio near 1.5 does indeed resemble Fig. 2(b). The dimension-lowering averaging described in the last paragraph also does not distinguish sharply, since small differences in the subset of phase-equal points can slightly displace average position. However, strobing at ω_h creates a single loop (ellipse in this case), unambiguously different from Fig. 5. An even more compelling distinction, which gives additional information about the torus, is a the half frequency (2π/doubled period) strobe. As indicated; the torus overlaps with itself, so the challenge is to distinguish which points are which. In Fig. 7 we show simulation images for two time periods. In each case the points selected on even numbered strobes are distinguished from odd-numbered strobes by symbol and color. For the Lissajous figure there is but a single loop or curve at each time; this is the third image of the figure.

IV. LONG TIME STABILITY

We have developed a number of tools for monitoring possible changes in the breather as a function of time. In situa-
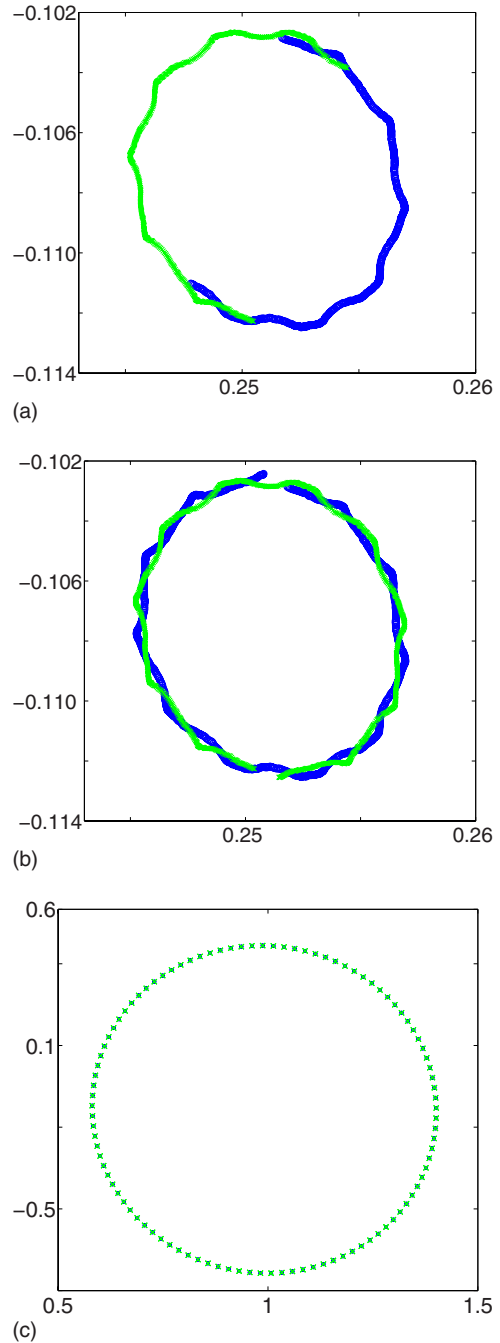

FIG. 7. (Color online) Strobing at the period doubled frequency ($\omega_\ell/2$). Images (a), (b) are for the dynamical simulation, with runs of 3000 and 5000 time units, respectively. Points are labeled according to whether they enter on odd or even numbered strobe images. For the shorter interval the torus has not filled out and the two portions have not quite met. For 5000 time units the torus has nearly filled out completely and it is clear that there are two separate portions. Image (c) is what one gets for the Lissajous figure, a combination of sines and cosines with frequencies 1.01 and 1.5, close to the 3-2 ratio.

tions where there is decay of the breather (such as "high" temperature), we find the most physically relevant quantity to be the gradual movement of the position of the inner envelope of breather oscillations (see [18] for discussion). By

contrast, what we now demonstrate is *stability*, and a more sensitive measure of the *lack* of change will be employed.

As noted earlier, in principle the breather in a diatomic lattice is not absolutely stable. This is because it possesses *two* principal frequencies, one in the gap between the acoustic and optical phonon bands, and one above the optical phonons. By virtue of the nonlinearity, higher harmonics of these frequencies are present and when (positive and negative) multiples add to match phonon frequencies, energy will radiate away from the breather, delocalizing it. What we show below is that despite this "in principle" argument, the breather that we obtain in our simulations is stable on any detectable time scale. We will also see that this is consistent with the suppressed intensities of higher harmonics for the breather.

The resonance argument does not apply if only one of the breather frequencies is excited. In fact there are extensive studies of gap-frequency breathers in diatomic lattices [19]. Moreover, it is true that the physical phenomenon we seek to explain (anomalous decay of luminescence) could be accounted for by a breather that initially has two frequencies, but for which one of them decays by resonance, leaving the other to survive. That would be enough to induce the slow crystal relaxation that we require. However, our previous numerical studies have suggested that even with two frequencies we get a considerable degree of stability, and it is this phenomenon we explore in the present paper.

Several measures of breather stability are not suitable. For example, the total energy in any finite subset of atoms will vary. Amplitudes are similarly difficult to get information from. Radiated energy (if there is any) is difficult to distinguish from either the exponential dropoff (with distance) in breather excitation or from residual excitation present even after we have done our best to create a pure breather.

What we have found is that the frequencies associated with the breather are extremely stable. They are very much functions of whatever one could define to be the breather amplitude, in the sense that they measure the extent to which this excitation is pushed into the nonlinear regime. They measure how steep the potential is for the amplitudes of interest.

Another way to look at this is in terms of action angle variables. If, in the sense of Kolmogrov-Arnold-Moser (KAM) theory, one has a Hamiltonian that has been put in the form $H(J_1, J_2)$, with the J's a measure of the action associated with this excitation, then the associated frequencies, $\omega_k = \partial H / \partial J_k$ are surrogates for the J's as indicators of stability.

A. Procedure for measuring frequency

The system is begun at rest (all q's, $\dot{q}$'s, Q's, and $\dot{Q}$'s zero) with the nonzero value of q_0 (the "push" from the Jahn-Teller distortion) forcing the system away from rest. For a preparatory period, typically 1000 or 1500 time units, the far end of the chain is dissipative. Thus a breather is formed with any nonbreather excitation radiated away and absorbed. After this, the profile, energy as a function of atom number, declined approximately exponentially. In addition, there were certain computational tricks, described in [18], to avoid coherent reflections off the far end of the chain. The amount of energy remaining after the radiation was a function of the parameters. For fixed ν and λ, as q_0 increased, this energy increased, although we did not see sudden changes, even in the neighborhood of the bifurcation discussed above (Sec. III).

Once the dissipation was turned off the system evolved under pure Hamiltonian dynamics for (typically) 5000 time units. This interval was broken into smaller times, from 200 to 1000 time units, and the dominant frequencies measured in a moving window with this width. Evaluation of the frequency used a method of Takatsuka [20]. Further details on the application of this method to our system can be found in [17].

B. Time dependence of the frequency

For the frequency data of Fig. 8, we used a moving window of width 900 time units, which is wide enough to give six-figure accuracy. This accuracy is possible with the method of Takatsuka when there is *a priori* reason to expect an isolated peak. It was checked for the recovery of frequencies on artificial data, using corresponding time intervals and mesh (Δt within the time intervals). We maintained six-figure accuracy despite the fact that the number of points in the fast Fourier transform was only 2^{12}, the time interval was 1000, and the size of the mesh was 0.1. It is the *a priori* assumption about quasimonochromaticity that allows one to do better than a naive uncertainty principle argument would suggest.

As is evident in Fig. 8, the frequencies hardly change at all. A linear fit gave slopes consistent with zero. We mention that in cases where the breather *is* decaying for one reason or another (e.g., when there is noise present, as in our finite-temperature studies), there is a clear response in the frequency dependence.

The high frequency breather shows a surprisingly slow periodicity in its tiny variation; we ascribe this to beating between (faster) modes of the system.

In an effort to understand the extreme stability against radiation, we checked whether combinations (sums of multiples with both positive and negative integer coefficients) of breather frequencies landed in the phonon bands. Even for $q_0 = 0.59$, the most nonlinear of the runs we are displaying, the smallest combination that lands in the phonon bands was $3(\omega_h - \omega_\ell)$, which fell into the range of the optical band. It is such combinations that would appear in nonlinear terms acting on the phonon modes, hence inducing radiation and decay of the breather.

The third harmonics of these breathers were down by many orders of magnitude, as can be seen in an extended version of Fig. 3. From a graph showing frequencies as large as $3\omega_h$, one can see that the intensity for the $3\omega_\ell$ terms is down nearly seven powers of 10, while the corresponding term for ω_h is down by more than seven powers of 10. It is thus completely reasonable that their effect is depressed at the level that we found.

Returning to the physical demands of our model, we can conclude from these data that the frequency is unchanging on
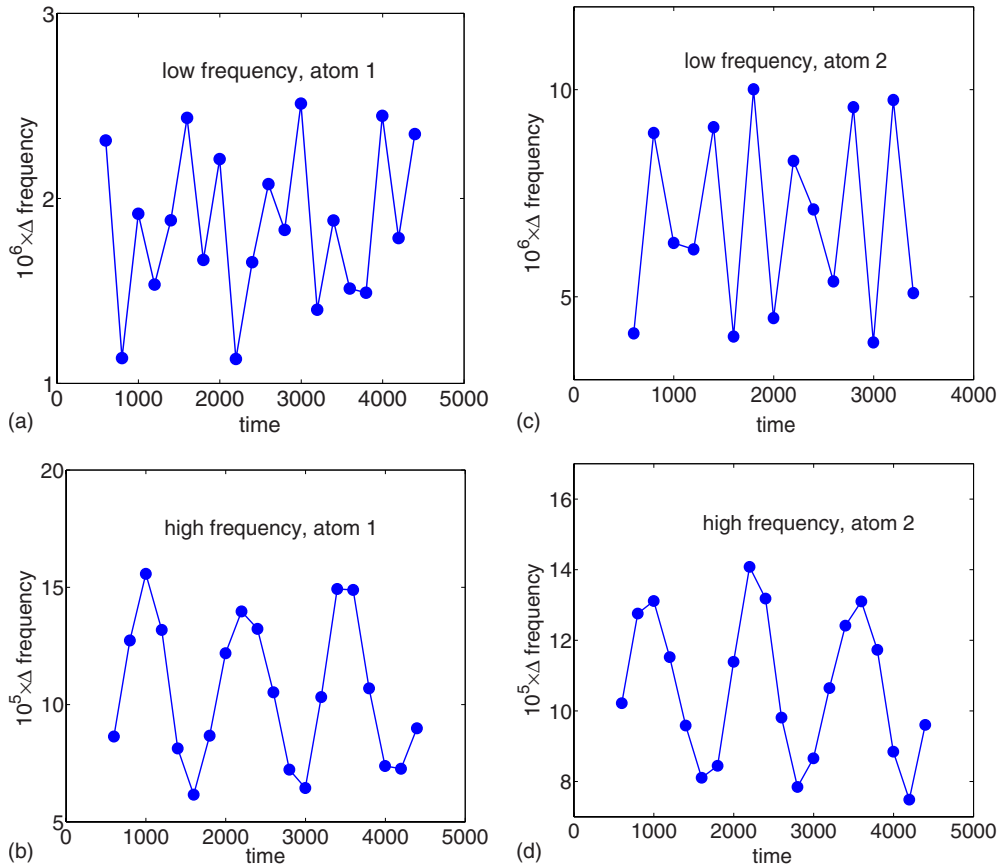
FIG. 8. (Color online) Breather frequencies for the first two atoms in a moving window of width 900 time units, for a run of 5000 time units. In each case a fixed frequency (given below) f is subtracted from the values in the graph. Note that the frequencies cluster in an extremely narrow range. We estimated their change in time with a linear fit, which gave us rates of change that were consistent with zero. Specifically we found that (slope, standard deviation) for the four cases graphed is (a) $(4.5657 \times 10^{-11}, 8.4086 \times 10^{-11})$, (b) $(-4.8344 \times 10^{-9}, 6.0324 \times 10^{-9})$, (c) $(5.3209 \times 10^{-11}, 9.8383 \times 10^{-11})$, (d) $(-3.97 \times 10^{-9}, 3.9778 \times 10^{-9})$. [For graph (a), the frequency displacement is $f_a = 1.927\,53$; similarly, $f_b = 2.8129$, $f_c = 1.79914$, $f_d = 2.8129$.]

a time scale of 10^9 units. This implies that the mechanism responsible for the anomaly in luminescence decay is not affected by the in-principle problem associated with multiple frequencies in the diatomic lattice. Moreover, we feel that it is remarkable that conclusions can be drawn on system behavior that deal with times that are five or more orders of magnitude longer than the actual computer runs.

V. CONCLUSIONS

Two themes were developed in this paper. In one we exhibited and explored a phenomenon that we call *torus doubling*. It should be clear from the 3-to-2 resonance of the nonlinear modes (hence the half frequency of their difference) that this period doubling is intrinsically multidimensional. Moreover, the dimension of phase space in which this takes place is not high and the basic structure—a torus—is common. Thus we do not expect this kind of bifurcation to be rare.

The second theme had both particular and general interest. The particular issue concerned a model we have proposed to explain an anomaly in the decay of luminescence in doped alkali halides. The experimental phenomenon requires

a slowdown of crystal relaxation by nine orders of magnitude relative to normal crystal relaxation time scales. Our model invokes the presence of a nonlinear localized mode closely related to discrete breathers. As such, these breathers must be stable for times on the order of 10^8 breather oscillation periods. This we established in the context of our model.

The general interest attached to this result is the fact that although discrete breathers have only rigorously been shown to be stable in monatomic lattices, having a single breather frequency, they may be important even in more complex lattices. Despite the in-principle resonances with phonon modes, in practice the breather may nevertheless survive for extremely long time periods. The key is presumably the low amplitude for higher harmonics that many discrete breather systems possess.

In terms of technique, our study of torus doubling involved stroboscopic images of the torus at numerous relevant frequencies. In addition we found it useful to average over some of those images in order to bring the space down by yet another dimension, allowing better visualization and tracking of the phenomenon.

For the stability study, our indicator was breather frequency, a variable conjugate to the classical action and as such a quantity that is also sensitive to changes in the

breather in the course of time. We were able to obtain remarkable accuracy in this quantity by means of a method of Takatsuka [20], in which the assumption that a frequency is isolated allows precision far greater than the uncertainty principle would suggest. The accuracy was also confirmed using artificial data.

[1] K. Polák, M. Nikl, and E. Mihóková, J. Lumin. **54**, 189 (1992).

[2] J. Hlinka, E. Mihóková, and M. Nikl, Phys. Status Solidi B **166**, 503 (1991).

[3] J. Hlinka, E. Mihóková, M. Nikl, K. Polák, and J. Rosa, Phys. Status Solidi B **175**, 523 (1993).

[4] E. Mihóková, M. Nikl, K. Polák, and K. Nitsch, J. Phys.: Condens. Matter **6**, 293 (1994).

[5] M. Nikl, J. Hlinka, E. Mihóková, K. Polák, P. Fabeni, and G. Pazzi, Philos. Mag. B **67**, 627 (1993).

[6] B. Gaveau, E. Mihóková, M. Nikl, K. Polák, and L. S. Schulman, Phys. Rev. B **58**, 6938 (1998).

[7] L. S. Schulman, E. Mihóková, A. Scardicchio, P. Facchi, M. Nikl, K. Polák, and B. Gaveau, Phys. Rev. Lett. **88**, 224101 (2002).

[8] L. S. Schulman, D. Tolkunov, and E. Mihóková, Phys. Rev. Lett. **96**, 065501 (2006).

[9] R. S. MacKay and S. Aubry, Nonlinearity **7**, 1623 (1994).

[10] D. K. Campbell, S. Flach, and Y. S. Kivshar, Phys. Today **57** (1), 43 (2004).

[11] In the Jahn-Teller effect, the distortion is symmetric along the symmetry-breaking axis. In other words, reflection symmetry with respect to the perpendicular plane is not broken. For the model it is therefore sufficient to use a ray emanating from the central Pb atom.

[12] E. Mihóková, L. S. Schulman, K. Polák, and W. Williams, Phys. Rev. E **70**, 016610 (2004).

[13] J. M. T. Thompson and H. B. Stewart, *Nonlinear Dynamics and Chaos: Geometrical Methods for Engineers and Scientists* (Wiley, Chichester, 1986).

[14] V. D. Barger and M. G. Olsson, *Classical Mechanics: A Modern Perspective*, 2nd ed. (McGraw-Hill, New York, 1995).

[15] D. Wilczak and P. Zgliczynski, e-print arXiv:0712.1123v1.

[16] This was done in Ref. [17], where the action was systematically calculated as a function of displacement of *both* first and second atoms.

[17] L. S. Schulman, Phys. Rev. A **68**, 052109 (2003).

[18] E. Mihóková and L. S. Schulman, "Noisy breathers and temperature-dependent luminescence decay" (unpublished).

[19] A. V. Gorbach and M. Johansson, Phys. Rev. E **67**, 066608 (2003).

[20] K. Takatsuka, J. Comput. Phys. **102**, 374 (1992).